JPn Neuroscience

The Journal of Physiology

J Physiol 592.13 (2014) pp 2785–2797

Rhodopsin in the rod surface membrane regenerates more rapidly than bulk rhodopsin in the disc membranes *in vivo*

Christopher Kessler[1], Megan Tillman[1], Marie E. Burns[2,4] and Edward N. Pugh Jr[3,4]

[1] *Center for Neuroscience, University of California, Davis, Davis, CA, USA*
[2] *Department of Ophthalmology and Vision Science, University of California, Davis, Davis, CA, USA*
[3] *Department of Physiology and Membrane Biology, University of California, Davis, Davis, CA, USA*
[4] *Department of Cell Biology and Human Anatomy, University of California, Davis, Davis, CA, USA*

Key points

- The early receptor potential (ERP) of the mouse electroretinogram (ERG) was measured in wild-type (WT) mice, in mice (*Opn1sw*$^{-/-}$) that lack S-cone opsin and overexpress M-cone opsin, and in mice heterozygous for the retinal pigment epithelium isomerase Rpe65.
- The amplitude of the ERP saturated exponentially with flash intensity. In WT mice the saturated amplitude was ∼1000 μV, about 20% larger than the saturated amplitude of the ERG a-wave.
- The ERP was 13% larger in mice overexpressing M-opsin than in WT mice, indicating that 26% of the ERP of WT mice in these experiments arises from M-opsin.
- After complete bleaching, the ERP of WT mice recovered in two phases, a fast phase responsible for ∼20% of the recovery having a time constant of ∼1 min, and a complementary slower phase with a time constant of 23 min. The fast phase of ERP recovery did not depend on the expression level of Rpe65, but the slow phase did.
- The fast phase of ERP recovery is concluded to arise from M-opsin regeneration, and the slow phase from the regeneration of rod plasma membrane rhodopsin. The slower phase of ERP recovery is faster than the regeneration of bulk rhodopsin in the internal disc membranes, consistent with the hypothesis that delivery of 11-*cis* retinal across the cytoplasmic gap between plasma and disc membranes retards regeneration of disc membrane rhodopsin.

Abstract Sustained vertebrate vision requires that opsin chromophores isomerized by light to the all-*trans* form be replaced with 11-*cis* retinal to regenerate the visual pigment. We have characterized the early receptor potential (ERP), a component of the electroretinogram arising from photoisomerization-induced charge displacements in plasma membrane visual pigment, and used it to measure pigment bleaching and regeneration in living mice. The mouse ERP was characterized by an outward 'R2' charge displacement with a time constant of 215 μs that discharged through a membrane with an apparent time constant of ∼0.6 ms. After complete bleaching of rhodopsin, the ERP recovered in two phases. The initial, faster phase had a time constant of ∼1 min, accounted for ∼20% of the total, and was not dependent on the level of expression of the retinal pigment epithelium isomerase, Rpe65. The slower, complementary phase had a time constant of 23 min in wild-type (WT) mice (C57Bl/6) and was substantially slowed in *Rpe65*$^{+/-}$ mice. Comparison of the ERPs of a mouse line expressing 150% of the normal level of cone M-opsin with those of WT mice revealed that M-opsin contributed 26% of the total WT ERP in these experiments, with the remaining 74% arising from rhodopsin. Thus, the fast regenerating fraction (20%) corresponds approximately to the fraction of the total ERP independently estimated to arise from M-opsin. Because both phases of the ERP recover substantially faster than previous measurements of bulk rhodopsin regeneration in living mice, we

© 2014 The Authors. The Journal of Physiology © 2014 The Physiological Society

DOI: 10.1113/jphysiol.2014.272518

conclude that delivery of the highly hydrophobic 11-*cis* retinal to the interior of rod photoreceptors appears to be retarded by transit across the cytoplasmic gap between plasma and disc membranes.

(Received 7 February 2014; accepted after revision 23 April 2014; first published online 6 May 2014)
Corresponding author E. N. Pugh: University of California, Davis, Physiology and Membrane Biology, 3301 Tupper Hall, 1 Shields Avenue, Davis, CA 95616, USA. Email: enpugh@ucdavis.edu

Abbreviations ERC, early receptor current; ERG, electroretinogram; ERP, early receptor potential; GPCR, G protein-coupled receptor; ISI, interstimulus interval; R1, initial, corneal-positive, component of the ERP; R2, second, corneal-negative, component of the ERP; Rpe65, retinal pigment epithelium isomerase; WT, wild-type.

Introduction

The early receptor potential (ERP) is a component of the electroretinogram that arises from charge displacements in opsin G protein-coupled receptors (GPCRs) (apo-opsin + 11-*cis* chromophore) that accompany the conformational changes consequent to chromophore photoisomerization (Brown & Murakami, 1964; Cone, 1964; Pak & Cone, 1964; Penn & Hagins, 1972; Rüppel & Hagins, 1973). The charge displacements underlying the ERP have also been recorded with single-cell methods as whole-cell currents (ERCs) or transmembrane potentials (ERPs) in native photoreceptor cells (Hodgkin & O'Bryan, 1977; Makino *et al.* 1991; Woodruff *et al.* 2004) and in cultured cells transfected with opsins (Sullivan & Shukla, 1999). Only opsins in the plasma membrane can contribute to an ERP or ERC, as internalized membranes such as the disc membranes of rods are electrically uncoupled from the surface membrane. In rodent retinas in which cones are relatively sparse, the ERP is generally thought to arise from rhodopsin molecules located in the plasma membrane of rod photoreceptors, including a contribution from newly formed basal discs that are continuous with the plasma membrane (Rüppel & Hagins, 1973).

Once light isomerizes the 11-*cis* chromophore to the all-*trans* form, restoration of the opsin GPCR to the resting, photoactivatable state requires that the all-*trans* chromophore be hydrolysed from its Schiff base linkage, and that a fresh 11-*cis* chromophore be delivered and covalently attached within the binding pocket (reviewed in Lamb & Pugh, 2004; Wang & Kefalov, 2011; Saari, 2012) – a process known as *regeneration*. For rods in mammalian retinas it is well established that the 11-*cis* chromophore that regenerates the bulk rhodopsin in the intracellular disc membranes is synthesized from the all-*trans* retinyl ester precursor in the retinal pigment epithelium by the isomerohydrolase RPE65 (Jin *et al.* 2005; Moiseyev *et al.* 2005). Regeneration of the bulk rhodopsin after a full bleach follows rate-limited kinetics *in vivo* (Lamb & Pugh, 2004), but the rate-limiting biological mechanism may be enzymatic or physical, and may be species specific (Lamb & Pugh, 2006). For example, in humans, the rate of 11-*cis* chromophore oxidation can limit the rate of regeneration (Cideciyan *et al.* 2000). Similarly, in some strains of mice, the rate of regeneration appears to be limited by the isomerohydrolase RPE65, since the maximal regeneration rate is dependent on the expression level of RPE65 over a nearly 10-fold range (Lyubarsky *et al.* 2005). However, recent work with isolated salamander rods suggests that the physical movement of chromophore across the cytoplasmic gap between the plasma membrane and disc membranes can limit the rate of regeneration (Frederiksen *et al.* 2012). Quantifying the recovery of the ERP after bleaching provides a potential means of testing this hypothesis in the living eye, and here we undertake such experiments.

Methods

Ethical approval

All mice were housed and handled according to a protocol approved by UC Davis Institutional Animal Care and Use Committee (IACUC) and in compliance with NIH guidelines for the use of animals in research. Mice were housed in standard 12 h/12 h dark/light cycles and dark-adapted overnight prior to experiments. Wild-type mice were C57Bl/6N obtained from Charles River (500 Park Center Drive, Hollister, CA 95023), or $Rpe65^{+/+}$ littermate controls generated in crossing heterozygous $Rpe65^{+/-}$ pairs. $Rpe65^{+/-}$ were genotyped as described in Redmond *et al.* (1998) and Lyubarsky *et al.* (2005). S-opsin knockout mice were created and characterized by Daniele *et al.* (2011), and genotyped as described in that study. All mice were between 3 and 5 months of age at the time of the experiments.

Electroretinography

Mouse experimental protocol, anaesthesia. Electroretinograms (ERGs) of mice that had been dark-adapted overnight were recorded with a customized apparatus (Fig. 1). For an experiment, anaesthesia was induced with 5% isoflurane, and then the mouse was placed on a platform with a custom bite bar that exposes the eye and holds the mouse's head firmly, and allows continuous delivery of 1.5% isoflurane in medical grade O_2 at a rate of 1–1.5 l min^{-1} through a nose cone. The mouse's

© 2014 The Authors. The Journal of Physiology © 2014 The Physiological Society

pupils were dilated with a 1% tropicamide solution, and wetted and kept moist with topical Goniovisc (2.5% hypromellose; HUB Pharmaceuticals, 9339 Charles Smith Ave., Building 150, Rancho Cucamonga, CA 91730). The body temperature of the mouse was maintained at 37°C by a heating pad (ATC-1000, WPI Inc.). In some experiments, a drop of 2.5% phenylephrine hydrochloride (Akorn, Inc.) was also applied, resulting in enhanced globe protrusion and improved electrical isolation of the corneal surface. Thus, phenylephrine was associated with a substantial increase in saturated ERP and a-wave amplitude, although there was no change in kinetics.

Electrical recording. ERGs were recorded with a customized platinum loop corneal electrode of inner diameter 1.5 mm and outer diameter 2.0 mm. The electrode formed an artificial pupil, and the surface facing the light source was coated with an opaque black enamel to minimize flash artifacts. A ground electrode was inserted subcutaneously in the forehead or neck. Responses were measured with a battery-operated differential amplifier (BMA-200, CWE Inc.) located near the mouse in a Faraday cage. Recordings were filtered at 1–30,000 Hz (4-pole Butterworth) and digitized at 153.8 kHz with a commercial USB A/D board (Digidata 1440, Molecular Devices Inc.), and epoch-capable acquisition software (pCLAMP 10.3, Molecular Devices Inc.).

Light delivery and calibration. Light flashes were generated with a xenon arc flash lamp (LF-1, Hamamatsu Inc.). The temporal distribution of the flash had a full-width half-maximum of ~5 μs (Fig. 1), much briefer than the predominant R2 component of the ERP. In most experiments, the flashes were delivered to the mouse via a 5 mm diameter fibre optic bundle that transmitted negligible ultraviolet light (Fig. 1*B*, black trace). The fibre optic tip was placed ~1 mm from the eye whose dilated pupil had a diameter of ~2.5 mm. As the adult mouse eye is approximately a sphere of diameter 3.2 mm and the nodal point of the eye is very near its centre (Remtulla & Hallett, 1985), the geometric image of the 5 mm diameter fibre optic tip would subtend a visual angle of $2 \times \tan^{-1}[(5/2)/(1 + 1.6)] \approx 90$ deg, if the image were in focus. However, because the normal C57Bl/6 mouse eye is nearly emmetropic (Remtulla & Hallett, 1985), the fibre optic will be too close to the eye to be in focus and consequently the xenon flash will illuminate most of the retina, though inhomogeneously. To obviate problems that might arise from spatial inhomogeneity in bleaching, we employed trains of unattenuated flashes to completely bleach all pigment underlying the ERP. Our experiments took advantage of the fact that the flash unit could generate identical flashes at repeat frequencies up to 30 Hz (data not shown). Assuming negligible regeneration in the 33 ms between flashes, the rate of decline of the ERP amplitude with flash number in a 30 Hz series lasting 1–20 s was used to estimate the fraction of pigment bleached per flash. In a subset of experiments the flashes were delivered via a liquid light guide that did pass UV as well as visible light (Fig. 1*B*, red trace).

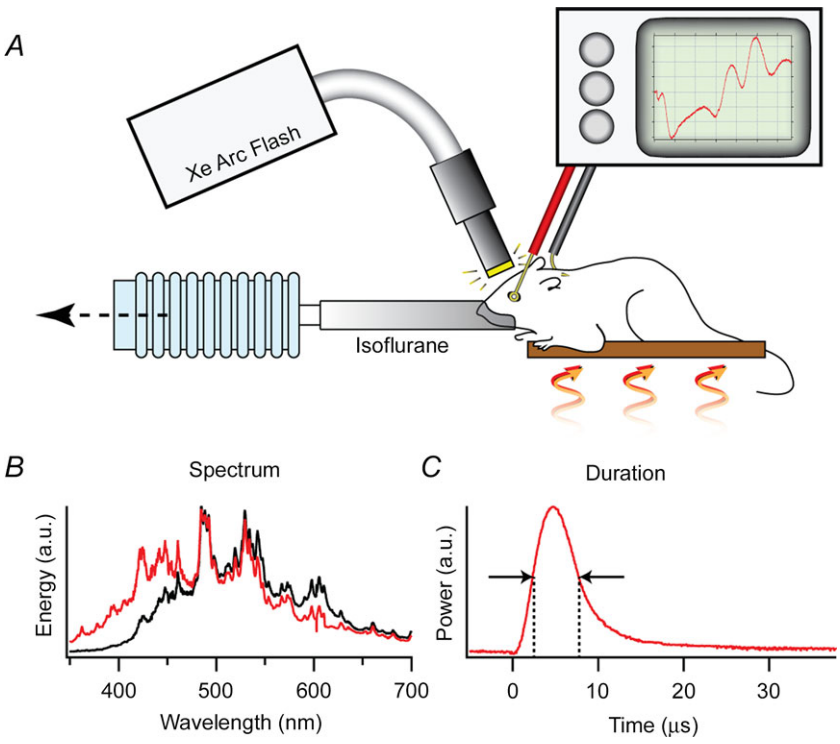

Figure 1. Description of the ERG apparatus and flash unit
A, the mouse was anaesthetized with 1.5% isoflurane delivered through a tube fitting snugly around its nose and held on an adjustable, heated platform. Light from a xenon flash unit was delivered to the eye by a 5 mm diameter fibre optic positioned ~1 mm from the corneal surface and normal to its centre of curvature. ERGs are recorded via a differential amplifier connected to a platinum ring corneal electrode and a reference electrode inserted subcutaneously into the forehead (Methods). *B*, spectral profiles of light delivered through the glass fibre optic bundle (black trace) and a liquid guide (red trace), measured with an Ocean Optics Inc (830 Douglas Ave, Dunedin, FL 34698) USB 2000 spectrometer with 0.3 nm resolution. *C*, the time course of the flash measured with Thorlabs Inc (56 Sparta Ave, Newton, NJ 07860) FDS010 photodiode with 1 ns rise time.

© 2014 The Authors. The Journal of Physiology © 2014 The Physiological Society

Kinetic model of ERP. Hodgkin & O'Bryan (1977) developed a model of the ERP and applied it to ERPs of turtle cones measured with intracellular electrodes.

The photoisomerization of N_Φ chromophores in the plasma membrane of a photoreceptor was assumed to generate a transient component of membrane current given by

$$j_\Phi(t) = -N_\Phi K\delta(t) + N_\Phi BKa_3 exp(-a_3 t) \qquad (1)$$

where K, B and a_3 are constants and $\delta(t)$ is the Dirac delta function. In the first term, $-K\delta(t)$ represents an effectively instantaneous inward charge movement corresponding to the R1 component of the ERC, while the second term represents an exponentially relaxing outward charge movement corresponding to the R2 component. The parameter B represents the ratio of the amplitude of the R2 to R1 current magnitudes, while $\tau_{R2} = 1/a_3$ is the time constant of the R2 current transient, and K is a proportionality factor relating each isomerization to charge movement during the R1 transition. The transmembrane potential change $\Delta V_m(t)$ induced by the current transient given by eqn (1) is readily derived by using $j_\Phi(t)$ as the forcing function for an isopotential cell with membrane time constant τ_m. The resultant total membrane current $J_{tot}(t)$ is the sum of the forcing current (eqn (1)) and the capacitive current. Taking into consideration that the flash is not impulsive, the total current is expressible (cf. Hodgkin & O'Bryan, 1977, eqn (31)) as

$$J_{tot} = \frac{N_\Phi K}{a_2}\left[\frac{a_1}{a_1 - a_2}[e^{-a_2 t} - e^{-a_1 t}]\right] + \frac{N_\Phi K}{a_2} \times \left[\frac{B\, a_1\, a_3[(a_2 - a_3)e^{-a_1 t} + (a_3 - a_1)e^{-a_2 t} + (a_1 - a_2)e^{-a_3 t}]}{(a_1 - a_2)(a_2 - a_3)(a_3 - a_1)}\right] \qquad (2)$$

where $1/a_1$ is the decay time constant of their flash and $a_2 = 1/\tau_m$. In our experiments the flash duration was very brief (see above) and the recording of sufficient bandwidth to allow resolution of the R1 transient. However, it can be shown that treating the flash as effectively instantaneous and the R1 transient as an exponential decay with a finite time constant results in the same formula as eqn (2), with $1/a_1 = \tau_{R1}$ reinterpreted as the R1 time constant. Equation (2) was fitted to normalized ERP traces by least squares minimization with scripts written in Igor Pro (WaveMetrics, 10200 SW Nimbus, G-7, Portland, OR 97223) and MATLAB (MathWorks, 3 Apple Hill Drive, Natik, MA 01760) to extract the parameters B, $\tau_{R1} = 1/a_1$, $\tau_{R2} = 1/a_3$ and $\tau_m = 1/a_2$. The factors K and N_Φ were lumped into a single scaling constant, and not independently estimated.

Flash artifact characterization and correction. The unattenuated (no neutral density ND = 0) xenon flash generated an electromagnetic artifact of typical amplitude 25 μV and time course that distorted the waveform of the ERP, particularly when the ERP amplitude was reduced by bleaching. To obviate the artifact, ERPs were normally recorded in response to a series of ND = 0 flashes lasting at least 1 s (and up to 20 s) presented at 30 Hz. As will be shown in the Results, such a train of flashes completely 'bleaches' the ERP, so that the traces obtained in response to the later flashes in the series record only the flash artifact, which was highly repeatable for a given experiment. By averaging 10 or more traces from the later portion of the train of flashes, a reliable measurement of the artifact for each experiment was obtained. The flash artifact, so measured, was then subtracted from the earlier traces in the series to obtain the artifact-corrected ERG/ERP.

Time course of ERP recovery following a complete bleach. The primary goal of the investigation was to measure the recovery of the ERP after completely bleaching the rhodopsin. The protocol employed for this purpose delivered two series of flashes at 30 Hz: the first series of up to 600 flashes delivered at 30 Hz reduced the ERP to zero, completely bleaching all rhodopsin; the second series of flashes, delivered after a prescribed time t between 1 and 60 min, was used to estimate the fraction of ERP recovery at time t, by means of the ratio of the amplitude of the artifact-corrected ERPs to the first flashes in each series. The recovery time course was describable as the sum of two independently recovering, exponentially rising, complementary components:

$$\mathrm{ERP}(t)/\mathrm{ERP}_{max} = 1 - C_1 \exp(-t/\tau_1) - C_2 \exp(-t/\tau_2). \qquad (3)$$

Here ERP_{max} is the amplitude of the ERP in response to the first flash in the initial bleaching series, $\mathrm{ERP}(t)$ is the amplitude of the response to the first flash in the flash series delivered at time t after the termination of the initial bleaching series, C_1 is the fraction of total pigment comprising one component and $C_2 = 1 - C_1$ the fraction comprising the complementary component, and τ_1 and τ_2 their respective time constants (expressed in minutes). Equation (3) was fitted to the ERP recovery data using custom scripts written in MATLAB and Igor Pro to find the parameters that minimized the mean squared error between the unweighted mean data points and the predicted values.

Steady-state bleaching/regeneration protocol. To quantify the regeneration of the rhodopsin at different steady-state bleach levels, the ERP was recorded in response to a series of identical unattenuated flashes delivered at interstimulus intervals (ISIs) ranging from 10 to 300 s, presented either after dark adaptation or immediately after a full bleach (600 unattenuated flashes, 30 Hz; Fig. 3). The normalized ERP amplitude typically reached a steady level within about 10 flashes (Fig. 6) and

© 2014 The Authors. The Journal of Physiology © 2014 The Physiological Society

was then used as a measure of the fraction of pigment (P) present when the rate of regeneration equalled the rate of bleaching. Thus, if we assume that each flash bleaches a constant fraction f_B of the pigment present, in the steady state the average rate of bleaching will equal the average *rate* of regeneration over the ISI epoch, and is given by

$$\text{Rate} = (f_B P)/\text{ISI} \quad (4)$$

The fraction bleached per flash (f_B) was estimated in the experiments described in Fig. 3 and Table 1.

Relative quantity of rod and cone pigments that contribute to the ERP

As the ERP arises only from pigment in the plasma membrane, and such pigment comprises only a small fraction of the total, it is useful to provide explicit estimates of the quantities of rod and cone opsins potentially contributing to the ERP in our experiments.

Rods. An average mouse rod outer segment has a length of 24 μm and diameter of 1.4 μm, with 41 discs μm^{-1} and an average of six 'patent' basal discs (i.e. discs continuous with the plasma membrane; Carter-Dawson & LaVail, 1979). The total rod outer segment membrane area calculated from these values is 3137 μm^2, with 126 μm^2 (3.9%) surface membrane (patent discs + cylindrical plasma membrane). Given that the density of opsin in the plasma membrane of rods has been estimated to be 30–50% that of the disc membranes (Kamps *et al.* 1982; Molday & Molday, 1987), the rhodopsin in the rod surface membrane that can contribute to the ERP is only 2% of the total rhodopsin.

Cones. Mouse cones are less numerous (1:33) and have smaller outer segments than mouse rods. An average mouse cone outer segment has a length of 13.4 μm, a base diameter of 1.2 μm tapering to a tip diameter of 0.8 μm, with 38 discs μm^{-1} (Carter-Dawson & LaVail, 1979). Unlike cold-blooded vertebrate cones whose disc membranes are all patent, mouse cones appear in electron micrographs to have only 25% of their discs patent (Carter-Dawson & LaVail, 1979), and presumably only this percentage can contribute to the ERP. Based on these values, the total mouse cone outer segment disc membrane area is ~800 μm^2, with an additional envelope surface membrane area of 44 μm^2. Thus, the total membrane surface area per cone is estimated to be $(800 \times 0.25) + 44 = 244$ μm^2, about twice that of a rod.

Given that cones comprise 3% of all C57Bl/6 photoreceptors (Carter-Dawson & LaVail, 1979; Jeon *et al.* 1998), then, the cone:rod ratio of total retinal outer segment membrane is $(244 \times 0.03)/126 = 0.059$, i.e. about 6%. Two additional factors come into play in assessing the potential contributions of cones *vs.* rods to the ERP in our experiments. The first is the density of opsins in the patent discs, which we assume to be the same for rods and cones. The second is that mouse cones express two different opsins, S-opsin ($\lambda_{max} = 360$ nm) and M-opsin ($\lambda_{max} = 510$ nm), with S-opsin predominant by a ratio of ~4:1 (Lyubarsky *et al.* 1999; Insinna *et al.* 2012). For experiments employing the glass fibre optic light guide that transmits negligible UV light (Fig. 1) and therefore activates only M-opsin, and, taking into consideration these two additional factors, we estimate the ratio of M-cone opsin to rhodopsin that could contribute to the ERP to be $(244 \times 0.03 \times 0.20)/(126 \times 0.5) = 0.02$, where 0.20 is the fraction of cone opsin that is M-opsin, and 0.5 is the relative density of rhodopsin in the plasma membrane.

Results

Properties of the early receptor potential and a-wave of the mouse ERG

The ERP and a-wave are both early appearing, corneal-negative components of the ERG elicited by a very bright flash, but are readily distinguished by their kinetics and their light dependence (Fig. 2). When a pair of identical intense flashes are delivered separated by a time interval of 100 ms, the initial flash triggers both ERP and a-wave components, while the second flash generates only an ERP, though of reduced amplitude (Fig. 2*A*). The ERP reaches its peak amplitude ~450 μs after the flash and is complete in less than 2 ms. In contrast, the a-wave is initiated near the termination of the ERP, peaking at around 4 ms from the onset of the flash. For flashes whose strengths were attenuated as much as 20-fold below the maximal attainable flash strength, the ERP and a-wave amplitude have totally distinct behaviour with respect to light intensity: the ERP amplitude depends strongly on the flash strength (Fig. 2*B* and *C*), while the a-wave amplitude is constant and saturated (Fig. 2*C*, open circles). The dependence of the ERP amplitude on flash intensity is well described by the exponential saturation relation originally applied by Cone (1964), who also found the saturating ERP amplitude to be approximately the same (1 mV) as that of the maximal a-wave in the rat. These differences between the a-wave and ERP reflect their distinct physiological origins: though both result from charge movements in the rod plasma membrane, the ERP arises from intramembrane charge movements accompanying the early conformational changes in isomerized photopigment molecules, while the a-wave arises from the suppression of the transmembrane rod circulating current as cGMP-activated channels close. It bears emphasis that the amount of visual pigment that can contribute to the ERP is only a small fraction of the total (Methods).

© 2014 The Authors. The Journal of Physiology © 2014 The Physiological Society

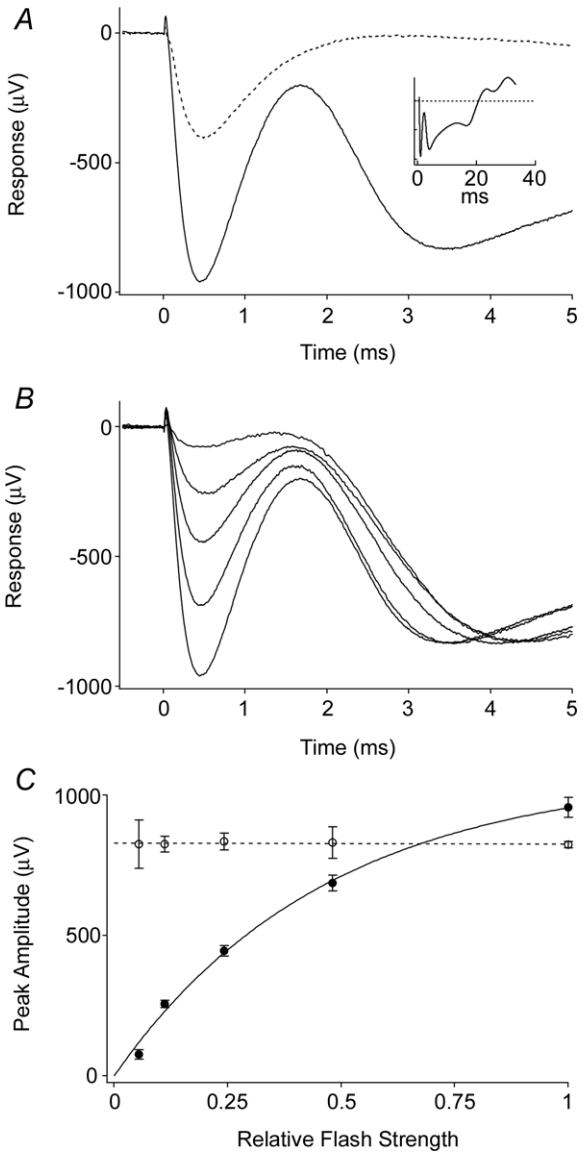

Figure 2. Properties of the mouse ERP
A, average ERG recorded in response to the first (continuous trace) and the second (dashed trace) of a pair of unattenuated flashes delivered 100 ms apart through the liquid light guide. The initial corneal-negative deflection, complete in ∼2 ms, is the ERP; it is followed in the first response by the corneal-negative a-wave, which does not recover between flashes. The amplitude of the second ERP is smaller, consistent with the first flash bleaching a significant fraction of the underlying pigment. Inset shows the first response on a longer time base. Each trace is the average from 5 experiments. *B*, average responses to first flashes that were attenuated incrementally by factors of ∼2. The initial ERP amplitudes varied with flash strength, while the a-wave amplitudes did not. Each trace is the average of 2–5 responses from separate experiments. *C*, initial ERP amplitude varied with flash strength. Average peak amplitudes of the ERP (filled circles) and a-waves (open circles) derived from the experiments of *B*. Each point is the mean ± SEM. (Phenylephrine was used in these experiments.)

Bleaching of the visual pigment underlying the ERP with flash trains

Trains of flashes delivered at 30 Hz were used to completely bleach the pigment underlying the ERP (Fig. 3). In response to successive flashes, the amplitude of the ERP declined in two phases, describable by a double-geometric depletion function:

$$\mathrm{ERP}(n) = \mathrm{ERP}_{\max}[A(1-P_A)^{n-1} + B(1-P_B)^{n-1}] \quad (5)$$

Here, $\mathrm{ERP}_{\max}$ is the amplitude of the initial ERP in the flash train, A and B represent the complementary fractions of the two distinct pools of pigment underlying the ERP (i.e. $A + B = 1$), $n = 1, 2, \ldots$ is the flash number, and P_A and P_B are the fractions of the respective pools depleted by each successive flash. The pool fractions were comparable for two different light guides (Methods), though the depletion rates were higher for the liquid light guide, reflecting greater light delivery (Table 1). One possible interpretation is that the two pools represent rhodopsin molecules in patent basal discs and in the cylindrical portion of the plasma membrane of rods, with different bleaching rates arising from the difference in chromophore dipole orientation with respect to axially propagating light. This interpretation is unlikely because the basal discs are expected to have *less* total pigment than the cylindrical plasma membrane (Methods) and to be at least 2-fold *more* sensitive to the light due to the pigment dichroism, whereas the more light-sensitive component comprises the major fraction of the total in our experiments (Table 1). A second possibility is that the light is distributed inhomogeneously over the retina, with the strength of illumination of two spatial pools standing in a ratio of roughly *A*:*B*. A third possibility is that the two pools represent rhodopsin and cone pigments, respectively, with the cone and rod pigments having indistinguishable ERP kinetics. Any contribution from the mouse UV-sensitive S-opsin can be excluded on the basis of the negligible UV content of the flash delivered with the glass fibre optic (Fig. 1*B*, black trace).

We tested the hypothesis that cone M-opsin contributes to the mouse ERP by recording ERPs from a mouse that lacks S-opsin (*Opn1sw*$^{-/-}$) and has an ∼50% increased expression of M-opsin (Daniele *et al.* 2011). The relative depletion pool sizes were not different between WT and S-opsin knockout (Table 1). However, the mean maximal ERP amplitude of the *Opn1sw*$^{-/-}$ mice was 13% greater ($P < 0.005$, Student's t test; Fig. 3) than that of the WT mice. This suggests that normally M-opsin contributes as much as 26% of the overall ERP of the WT mouse, with rhodopsin in the rod plasma membrane accounting for the remaining 74%. The value 26% is obtained by assuming that only rhodopsin and M-opsin contribute

© 2014 The Authors. The Journal of Physiology © 2014 The Physiological Society

to the ERP, and that rhodopsin expression is the same in WT and *Opn1sw*$^{-/-}$ mice. Thus, for WT mice the fractional contributions of rhodopsin (f_{Rho}) and M-opsin ($f_{\mathrm{M\text{-}ops,WT}}$) sum to unity, $f_{\mathrm{Rho}} + f_{\mathrm{M\text{-}ops,\,WT}} = 1$. For the *Opn1sw*$^{-/-}$ mice with a 1.5-fold greater expression of M-opsin and a 13% larger ERP, the corresponding sum is $f_{\mathrm{Rho}} + 1.5 f_{\mathrm{M\text{-}ops,WT}} = 1.13$, yielding $f_{\mathrm{M\text{-}ops,WT}} = 0.26$.

The value 26% is more than 10-fold greater than the contribution of M-opsin to the ERP (2%) predicted from analysis of the relative numerosity and structures of rods and cone outer segments (Methods). This discrepancy could arise if a larger fraction of cone discs were patent than estimated from electron microscopy data and if the amount of surface rhodopsin is overestimated. The estimated fraction of ERP signal contributed by M-opsin (26%) is comparable to the 'slowly depleting' fraction (Table 1, fraction '*B*', 15–21%), which appears to lend support to the hypothesis that the slowly depleting component of the ERP in the serial bleaching might arise from M-opsin. However, assuming that cone M-opsin is isomerized at least as effectively as plasma membrane rhodopsin and that cone opsin regeneration is negligible during the short (33 ms) interflash interval, M-opsin could not be depleted at a rate 20-fold slower than rhodopsin. Thus, it is unlikely that the slowly depleting fraction seen in serial bleaching arises from M-opsin bleaching and the similarity of these two numbers is probably a coincidence.

Because spatial inhomogeneity of light delivery must exist (Methods), we designed the experiments to characterize the regeneration of the ERP only after completely bleaching both pools of visual pigment using long trains of bright flashes (30 Hz, ND0 600 flashes). Given that the two pools contributing to the ERP have bleach rates of $P_A = 0.4$ and $P_B = 0.02$ per unattenuated flash, a train of 200 flashes will leave no more than $(1 - 0.4)^{200} < 10^{-44}$ and $(1 - 0.02)^{200} = 0.018$ in the rapidly and slowly depleting pools, respectively. Clearly, such a 'bleaching train' is sufficient to completely deplete both pools of photopigment underlying the ERP.

Kinetics of the mouse ERP: membrane time constant and time constants of the R1 and R2 transitions

The mouse ERP was well described by a slightly modified version of the model developed by Hodgkin & O'Bryan (1977) to characterize turtle cone ERPs (Fig. 4; Methods, eqn (2)). ERPs were averaged across 160 experiments, with each of the successive responses to the flashes in the 30 Hz bleaching train separately averaged. The theoretical model best fitting the data had time constants $\tau_{R1} = 46\ \mu$s, $\tau_{R2} = 215\ \mu$s and $\tau_m = 570\ \mu$s (Fig. 4*A*, red traces). The theoretical traces for responses 2–6 fall within the 95% confidence intervals of the data (grey region in Fig. 4*B*), and gauged by their negligible deviation from the theory trace, are invariant in shape. Notably, however, the initial ERP (trace 1) deviated highly reliably upward between 1.0 and 1.5 ms from the prediction of the model best-fitting the other traces (see arrows in Fig. 4*A* and *B*). The upward

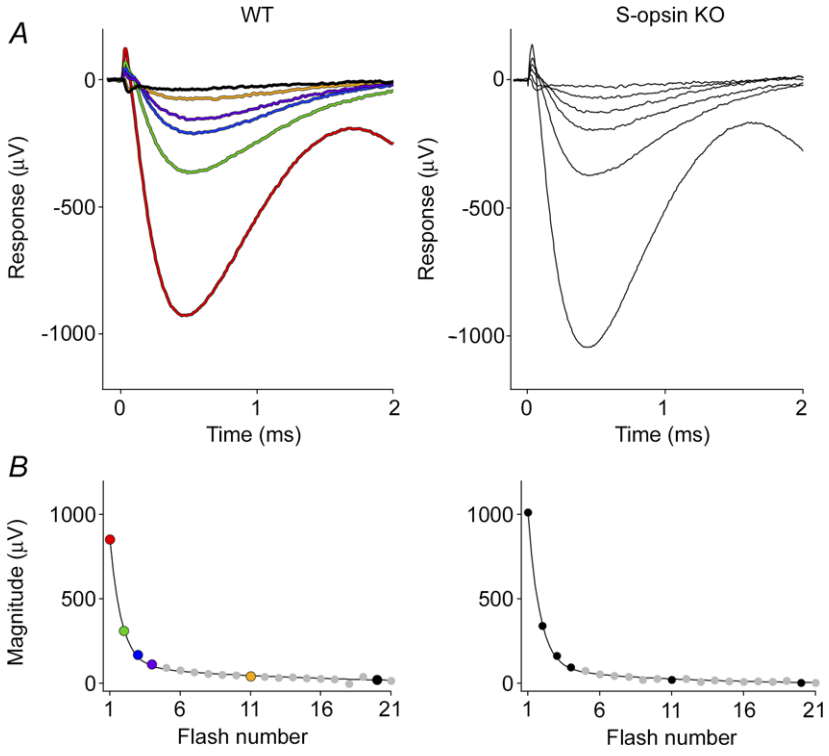

Figure 3. ERP serial bleaching of wild-type mice, and mice lacking cone S-opsin
A, the two upper panels show the first 2 ms of ERGs obtained in response to the first six of a series of unattenuated flashes delivered through the liquid light guide at 30 Hz. Both WT and S-opsin knockout (KO) data are averaged traces ($n = 5$ and 3, respectively). The amplitudes of the ERPs in response to the first flash were 924 ± 30 and 1042 ± 28 μV (mean ± SEM, $P < 0.005$), and 809 ± 27 and 813 ± 22 μV for the initial a-waves of the WT and the S-opsin KO, respectively. *B*, the lower panels plot the amplitude of the ERP as a function of the number of the flash in the series. The parameters of the best-fitting double-geometric depletion model (eqn (5)) are as follows: for the WT, $A = 0.87$, $P_A = 0.70$, $P_B = 0.07$; for the S-opsin KO, $A = 0.90$, $P_A = 0.71$, $P_B = 0.11$.

© 2014 The Authors. The Journal of Physiology © 2014 The Physiological Society

Table 1. Parameters characterizing decline of ERP with successive flashes

Parameter	A	B	P_A	P_B
Liquid light guide (WT)	0.85 ± 0.05	0.15 ± 0.12	0.71 ± 0.02	0.08 ± 0.02
Liquid light guide (*Opn1sw*$^{-/-}$)	0.90 ± 0.03	0.10 ± 0.16	0.71 ± 0.01	0.10 ± 0.01
Glass fibre optic (WT)	0.79 ± 0.02	0.21 ± 0.02	0.40 ± 0.05	0.02 ± 0.003

A and B represent complementary fractions of the initial ERP amplitude which are depleted at the rates P_A and P_B, respectively, by successive unattenuated flashes delivered via either the liquid light guide or the glass fibre optic (Methods) to the dark-adapted eye at 30 Hz (eqn (5)). The parameter values for the liquid guide were estimated from the WT data of Fig. 3*B* ($n = 5$), while those for the glass fibre optic were obtained from analysis of a randomly selected subset ($n = 16$) from 160 experiments. The error terms in the table are SEMs. The average fraction bleached by a single flash to the dark-adapted eye or in a steady-state level of regeneration was estimated as $f_B = (A \times P_A) + (B \times P_B)$.

direction of this deviation is opposite to that expected if it were due to intrusion of the a-wave. (The expected downward deviation arising from a-wave intrusion begins to occur around 1.5 ms.) The upward deviation can be characterized as arising from cells with an ∼15% shorter membrane time constant in their response to the first flash in the train. A possible explanation is that the first ERP has a substantial contribution from M-opsin-expressing cones that is largely eliminated by the first flash. This hypothesis is qualitatively inconsistent with our finding that the time constant of the ERP to the first flash is shorter than that to the second and subsequent flashes, because cones of a given species usually have a longer membrane time constant than rods (Schneeweis & Schnapf, 1999). The hypothesis is also quantitatively inconsistent with our estimate (26%) of the M-opsin contribution, as the initial flash in these experiments reduced the ERP amplitude by 40% (Table 1). We thus conclude that the most likely explanation is that the change in membrane time constant between the first and second flashes arises from sustained, light-dependent closure of rod cyclic nucleotide-gated channels, with a consequent increase in the rod membrane time constant.

Two phases of ERP recovery following a full bleach

After exposure to a full bleaching train, the ERP recovered its amplitude along a biphasic trajectory (Fig. 5). The overall time course of ERP regeneration could be described as the sum of two independent, exponentially recovering components, representing two complementary fractions of the total regenerating pigment (Fig. 5*A*; Methods, eqn (3)). The component fractions of the best-fitting two-phase model were $C_1 = 0.21$ and $1 - C_1 = 0.79$, respectively, with respective time constants $\tau_1 = 0.95$ min and $\tau_2 = 23.3$ min (red curve). Exploration of the parameter space $\{(C_1, \tau_1, \tau_2)\}$ near the best-fitting values revealed tradeoffs between the parameters in the fitting. Thus, the recovery data of the wild-type mice could be reasonably well fitted (RMS error within 10% of the global minimum) by a number of curves with different parameter values in the ranges $\{0.15 \leq C_1 \leq 0.30$; $0.55 \text{ min} \leq \tau_1 \leq 1.9 \text{ min}$; $21 \text{ min} \leq \tau_2 \leq 26 \text{ min}\}$. Overall, we conclude that the photopigment underlying the mouse ERP appears to comprise two pools whose relative sizes are between 1:5 and 1:3, and which regenerate with respective time constants of about 0.5–2 min and 20–30 min, respectively, after being fully bleached.

The rate of regeneration of 'bulk' rhodopsin (i.e. that residing in intracellular discs) in unanaesthetized mice depends on the level of expression of the RPE-specific isomerase Rpe65 (Lyubarsky *et al.* 2005). The presence of a distinct isomerase in Müller cells (Kaylor *et al.* 2013) that can supply 11-*cis* retinol for the regeneration of bleached cone opsins (Wang & Kefalov, 2009, 2011) raises the possibility that this second isomerase could contribute to the regeneration of the pigment whose isomerization underlies the ERP. To test this idea we measured the recovery of the ERP in *Rpe65*$^{+/-}$ C57Bl/6 mice, who have a 30% reduction in Rpe65, and comparatively slowed bulk rhodopsin regeneration that is 55% that of WT (*Rpe65*$^{+/+}$ C57Bl/6) (Lyubarsky *et al.* 2005). The *Rpe65*$^{+/-}$ mice had smaller ERP amplitudes at late times, though the initial, fast phase of ERP recovery was normal (Fig. 5*A*). These results indicate that Rpe65 and thus the retinal pigment epithelium is the dominant source of 11-*cis* retinal for the slow phase of ERP recovery, and suggest that another independent source, perhaps the Müller cells, could underlie the fast phase of ERP regeneration.

Regeneration rate is dependent on the extent of bleaching

The normal regeneration of rhodopsin may be rate-limited by enzymatic activities within the visual cycle or by the diffusional delivery of chromophore through a resistance (Lamb & Pugh, 2006). If enzymatic mechanisms are rate limiting, light history might alter the observed rate by affecting the enzymes that contribute to 11-*cis* retinal synthesis (Wenzel *et al.* 2005). To test whether the time course of pigment regeneration is affected by the light history, we used a repeated flash protocol to assess ERP amplitude at different steady-state levels

© 2014 The Authors. The Journal of Physiology © 2014 The Physiological Society

of pigment bleaching (Fig. 6). In these experiments, a flash that produced a maximal ERP amplitude was presented repeatedly at different interstimulus intervals (ISIs) ranging from 10 to 300 s. The steady-state amplitude achieved for each ISI was evaluated from two opposite initial conditions: the fully dark-adapted mouse (pigment pools initially full) or the fully bleached (pigment pools depleted).

ERP amplitudes in these experiments reached steady-state levels that varied with ISI (Fig. 6*B*). The longest ISI (300 s) resulted in little change in the ERP amplitude, with shorter ISIs producing progressively smaller steady-state amplitudes. For each ISI the steady-state ERP amplitude reached was very nearly the same regardless of whether the pigment pools were initially full or completely depleted (Fig. 6*A* and *B*, light *vs.* dark symbols). Assuming that the steady-state amplitudes reflect the equilibrium level of pigment in the surface membranes of photoreceptors and that the

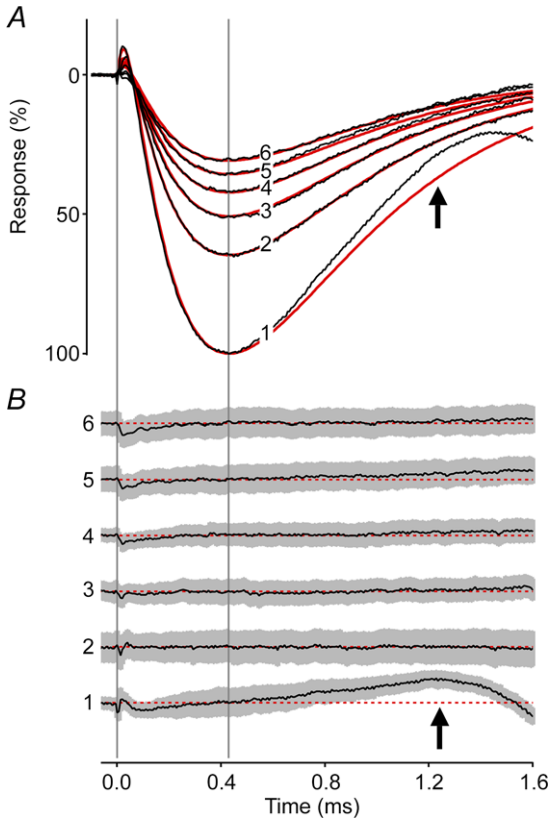

Figure 4. Invariant kinetics of the mouse ERP
A, the first 6 ERPs from a series of unattenuated flashes (30 Hz), averaged over 160 experiments (black traces). The red traces are the best-fitting version of a theoretical model (Hodgkin & O'Bryan, 1977; Methods, eqn (2)) with parameter values $\tau_{R1} = 46$ μs, $\tau_{R2} = 215$ μs and $\tau_m = 570$ μs. *B*, residual differences between the data and theory traces in *A* plotted along with the 95% confidence interval (grey region). The difference traces have been arbitrarily offset vertically from one another, but are plotted at the same scale as in *A*, and are identified at left with the corresponding numbers. The dashed red lines indicate the zero difference levels. A single set of kinetics parameters fitted the sequential responses well; the deviation of the initial ERP from the model (black arrows) is consistent with a shorter membrane time constant governing the ERP response to the first flash (see text).

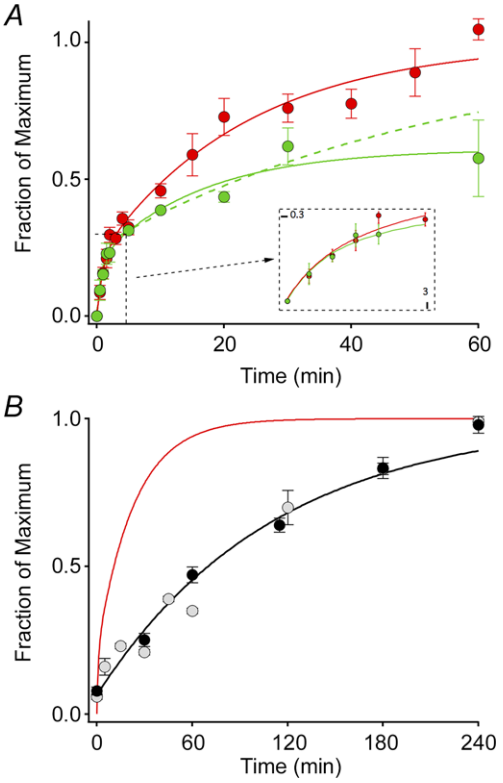

Figure 5. Time course of recovery of the ERP after a full bleach
A, ERP recovery. Each point represents the mean (± SEM) maximal ERP amplitude following a full bleach (600 unattenuated flashes, 30 Hz) and variable periods of dark adaptation. The red filled circles plot the data of WT mice ($n = 6$–13), while the green filled circles show the data of *Rpe65*$^{+/-}$ mice ($n = 3$–5). The continuous curves fitted to the data are double-exponential rises (eqn (4), Methods) with $C_1 = 0.21$, $\tau_1 = 0.94$ and $\tau_2 = 23.3$ min for the data of WT mice, and $C_1 = 0.21$, $\tau_1 = 0.84$ min and $\tau_2 = 16.4$ min for those of the *Rpe65*$^{+/-}$ mice. The recovery of the *Rpe65*$^{+/-}$ mice achieved only 61% recovery at 60 min, and the precise time course of the recovery, while clearly slowed, is poorly determined. Assuming (as established by experiments on subsequent days) full recovery, we forced the regeneration to asymptote to unity, yielding the dashed green curve, with parameters $C_1 = 0.25$, $\tau_1 = 0.84$ min and $\tau_2 = 56$ min. The inset shows the initial 3 min of recovery on an expanded time base. *B*, comparison of the ERP recovery (red trace, copied from *A*) with the regeneration of total rhodopsin of C57Bl/6 mice after a full bleach, replotted from two independent studies (pale symbols, Wenzel *et al.* 2001; black symbols and rate-limited regeneration time course from Lyubarsky *et al.* 2005). For the a-wave recoveries the same initial bleach protocol was used as in Fig. 3 (600 flashes, 30 Hz), but the subsequent test flash was attenuated 16-fold (ND = 1.2), and delivered every 2 min; flashes of this strength saturated the a-wave amplitude in the dark-adapted mouse. (All experiments in this figure were done with flashes delivered by the glass fibre optic light guide.)

© 2014 The Authors. The Journal of Physiology © 2014 The Physiological Society

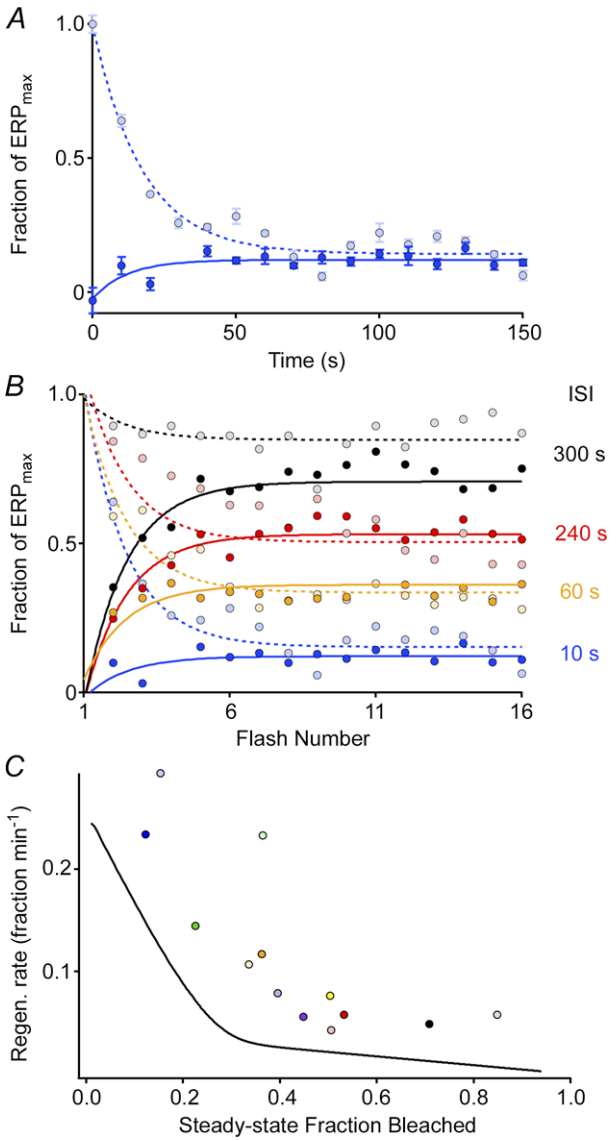

Figure 6. ERP regeneration rates measured in a steady-state, periodic flash protocol
A, ERP amplitude plotted as a function of flash number in experiments in which the unattenuated flash was delivered every 10 s, beginning either from a fully bleached state (dark blue filled circles) or beginning in the dark-adapted state (light blue filled circles); each point plots the mean (± SEM) from 3–4 experiments. *B*, results of experiments following the same protocol as in *A*, but with various interstimulus intervals (ISIs). Each point plots the mean from 3–4 experiments. All experiments used the glass fibre optic for light delivery. *C*, rates of regeneration (symbols) extracted from the final, steady-state levels in panel *B* using the same colour scheme (Methods, eqn (4), with $f_B = 0.32$; cf Table 1) plotted as a function of the steady-state fraction bleached, taken to be $1 - (ERP_{ss}/ERP_{max})$. (Data from 3 sets of experiments with ISIs of 30 s, 120 s and 180 s, which were not included in panel *B*, have been included in panel *C*). The continuous black curve plots the instantaneous rate of regeneration at each level $P(t)$ of the regeneration of the ERP following a full bleach, obtained as the derivative of the smooth curve fitted to the regeneration data (WT data) of Fig. 5*A*.

fraction bleached by each flash is a constant, each ISI experiment yields an estimate of the regeneration rate as a function of the steady-state fraction bleached (Methods, eqn (4)).

To further test whether the rates of regeneration of the pigment underlying the ERP varied with light history, we compared the instantaneous rates of regeneration at each time point in the ERP recovery following a full bleach (Fig. 5*A* and *B*, red curve) to the rates associated with each steady-state ERP amplitude in the ISI experiments (Fig. 6*C*, smooth curve *vs.* symbols).

It can be generally expected that the 2nd-order reaction governing regeneration of a specific opsin would approximately obey the relation

$$dP/dt = k[11\text{-}cis](1 - P) \quad (6)$$

where P is the fraction of pigment present, [11-*cis*] is the local concentration of 11-*cis* retinal and k a 2nd-order rate constant. Thus, if [11-*cis*] is constant one would expect the rate of ERP regeneration to be proportional to the fraction bleached, i.e. $1 - P$. (This oversimplifies the situation, as the unregenerated opsin can exist in transient intermediate metarhodopsin states in which the all-*trans* remains covalently attached.) Estimating $1 - P$ as $1 - (ERP_{ss}/ERP_{max})$, where ERP_{ss} is the steady-state amplitude of the ERP. In Fig. 6*C* we plot the regeneration rates (symbols) estimated from the data in Fig. 6*B* as a function of the fraction bleached, along with the rates (continuous line) estimated from the ERP regeneration data of Fig. 5. From these results we draw two conclusions. First, the ERP regeneration in both experiments is qualitatively similar, revealing two distinct components. Thus, there are two regions of similar and roughly constant slope. Each region can be understood as corresponding to a distinct rate constant k[11-*cis*] in eqn (6). Second, by the time the steady state is reached in the ISI experiments, the rates of regeneration are very similar regardless of whether they were measured starting from the dark-adapted *vs.* the fully bleached state. On the other hand, the discrepancy between the rates determined from the steady-state regeneration experiments (Fig. 6*C*, symbols) and the experiments in which regeneration proceeds uninterruptedly (continuous line) suggests the possibility that the prolonged light exposures in the ISI protocol may have increased the rate of regeneration (Wenzel *et al.* 2005).

Discussion

Use of the ERP to measure pigment regeneration *in vivo*

R. A. Cone (1964) showed directly that the amplitude of the rat ERP was directly proportional to the quantity

© 2014 The Authors. The Journal of Physiology © 2014 The Physiological Society

of rhodopsin bleached over a wide range of flash intensities. Like the original investigation by Cone, our results show that the mouse ERP amplitude saturates exponentially with flash strength (Fig. 2), and that the saturated amplitude can exceed that of the a-wave. To our knowledge, this is the first investigation to quantitatively compare the time course of recovery of the ERP measured *in vivo* with the time course of bulk rhodopsin regeneration *in vivo* of the same rod-dominant species. Previous investigations have, however, employed the ERP to measure the regeneration of cone visual pigment *in vivo* (Goldstein, 1969; Goldstein & Berson, 1969). For the discussion to follow, it bears emphasis that because the ERP originates solely from opsins in the plasma membrane, the fraction of the pigment that contributes to the ERP is only a few per cent of the total in the retina (Methods).

The mouse ERP has a substantial contribution from cones

Work in the 1960s on the rodent ERP characterized it as arising from rhodopsin in the rod plasma membrane (see Introduction). Since that time it has been well established that mice have cones which express short (S-) and mid-wave (M-) opsins (λ_{max} = 360 nm and 510 nm, respectively). Three distinct results in our experiments, obtained under conditions that largely eliminate contributions from S-opsin, indicate that about a quarter of the ERP of WT mice arises from cone M-opsin. The first result is that the amplitude of the ERP of a mouse line lacking S-opsin (*Opn1sw*$^{-/-}$) but expressing 50% more M-opsin (Daniele *et al.* 2011) is 13% larger than the WT ERP (Fig. 3); this result yields an estimate of 26% for the M-opsin contribution. The second result is that ∼20% of the ERP recovers with a time constant of ∼1 min after a complete bleach, a time constant close to that (1.3 min) of the recovery of cone sensitivity in the isolated mouse retina following bleaching (Kolesnikov *et al.* 2011). A third result is that this fast recovering component does not depend on Rpe65 (Fig. 5). The lack of dependence of the fast phase of ERP recovery on Rpe65 expression level is consistent with the hypothesis that the isomerase in Müller cells, dihydroceramide desaturase 1 (DES1) (Kaylor *et al.* 2013), which generates 11-*cis* retinol that cones can use for pigment regeneration (Ala-Laurila *et al.* 2009; Wang *et al.* 2009; Wang & Kefalov, 2009; Kolesnikov *et al.* 2011; Wang & Kefalov, 2011), may underlie the fast phase of regeneration of the ERP. The apparent contribution of M-cone opsin to the ERP substantially exceeds that expected from a simple calculation (0.03 M-opsin to total surface pigments) based on the anatomy of rods and cones and the numbers of patent discs in each (Methods). This suggests that basic assumptions like the number of patent discs and the expected pigment densities in the surface membranes are incorrect for mouse photoreceptors, and will be an important topic for future study.

An alternative (and not mutually exclusive) hypothesis for explaining the rapidly regenerating component of the ERP is that there is a small pool of 11-*cis* retinal not bound to opsins and that this pool is rapidly mobilized once the all-*trans* chromophore is hydrolysed from plasma membrane opsins. Such a pool could be free 11-*cis* retinal solubilized directly in the photoreceptor membrane (Azuma *et al.* 1977), or 11-*cis* retinal bound to cellular retinal binding protein (CRALBP) or interstitial retinoid binding protein (IRBP).

Plasma membrane rhodopsin regenerates more rapidly than disc membrane rhodopsin

Nonetheless for the contribution from cone pigment, the mouse ERP in our experiments is generated predominantly by rod surface membrane rhodopsin (74% of the total ERP amplitude). Consistent with this interpretation, the value of the membrane time constant of the photoreceptors underlying the ERP in our experiments (τ_m = 570 μs) is close to previous estimates from rodent rods of ∼1 ms (Penn & Hagins, 1972; Rüppel & Hagins, 1973). In contrast, had cones contributed a large fraction of the ERPs, we might expect τ_m to be substantially greater (Schneeweis & Schnapf, 1999).

After a full bleach, the plasma membrane rhodopsin underlying the more slowly recovering component of the ERP regenerates much more rapidly than the bulk rhodopsin that is predominantly in the discs (Fig. 5*B*). Bulk rhodopsin regeneration in humans, mice and other species follows rate-limited kinetics and it has been hypothesized that the rate limitation arises from an enzymatic rate limit, or from a biophysical limitation to the delivery of 11-*cis* retinal to the rod disc membranes (Lamb & Pugh, 2004, 2006). Recently, it has been shown in isolated salamander rods that the delivery of chromophore across the cytoplasmic gap separating the plasma and disc membranes limits the rate of regeneration (Frederiksen *et al.* 2012). The more rapid recovery of the dominant component ERP than bulk regeneration suggests that the regeneration of photopigments on the rod surface membrane is much faster than that of the bulk rhodopsin confined within intracellular discs (Fig. 5*B*), supporting the hypothesis that a diffusional or biophysical bottleneck can substantially limit the rate of chromophore delivery to mammalian rods (Frederiksen *et al.* 2012). Another factor that could contribute to more rapid regeneration of rhodopsin in the plasma membrane is a relatively faster rate of chromophore hydrolysis, a step that must occur before 11-*cis* retinal can recombine with the apo-opsin to form a visual pigment.

© 2014 The Authors. The Journal of Physiology © 2014 The Physiological Society

References

Ala-Laurila P, Cornwall MC, Crouch RK & Kono M (2009). The action of 11-*cis*-retinol on cone opsins and intact cone photoreceptors. *J Biol Chem* **284**, 16492–16500.

Azuma K, Azuma M & Sickel W (1977). Regeneration of rhodopsin in frog rod outer segments. *J Physiol* **271**, 747–759.

Brown KT & Murakami M (1964). A new receptor potential of the monkey retina with no detectable latency. *Nature* **201**, 626–628.

Carter-Dawson LD & LaVail MM (1979). Rods and cones in the mouse retina. I. Structural analysis using light and electron microscopy. *J Comp Neurol* **188**, 245–262.

Cideciyan AV, Haeseleer F, Fariss RN, Aleman TS, Jang GF, Verlinde CL, Marmor MF, Jacobson SG & Palczewski K (2000). Rod and cone visual cycle consequences of a null mutation in the 11-*cis*-retinol dehydrogenase gene in man. *Vis Neurosci* **17**, 667–678.

Cone RA (1964). Early receptor potential of the vertebrate retina. *Nature* **204**, 736–739.

Daniele LL, Insinna C, Chance R, Wang J, Nikonov SS & Pugh EN Jr (2011). A mouse M-opsin monochromat: retinal cone photoreceptors have increased M-opsin expression when S-opsin is knocked out. *Vision Res* **51**, 447–458.

Frederiksen R, Boyer NP, Nickle B, Chakrabarti KS, Koutalos Y, Crouch RK, Oprian D & Cornwall MC (2012). Low aqueous solubility of 11-*cis*-retinal limits the rate of pigment formation and dark adaptation in salamander rods. *J Gen Physiol* **139**, 493–505.

Goldstein EB (1969). Contribution of cones to the early receptor potential in the rhesus monkey. *Nature* **222**, 1273–1274.

Goldstein EB & Berson EL (1969). Cone dominance of the human early receptor potential. *Nature* **222**, 1272–1273.

Hodgkin AL & O'Bryan PM (1977). Internal recording of the early receptor potential in turtle cones. *J Physiol* **267**, 737–766.

Insinna C, Daniele LL, Davis JA, Larsen DD, Kuemmel C, Wang J, Nikonov SS, Knox BE & Pugh EN Jr (2012). An S-opsin knock-in mouse (F81Y) reveals a role for the native ligand 11-*cis*-retinal in cone opsin biosynthesis. *J Neurosci* **32**, 8094–8104.

Jeon CJ, Strettoi E & Masland RH (1998). The major cell populations of the mouse retina. *J Neurosci* **18**, 8936–8946.

Jin M, Li S, Moghrabi WN, Sun H & Travis GH (2005). Rpe65 is the retinoid isomerase in bovine retinal pigment epithelium. *Cell* **122**, 449–459.

Kamps KM, De Grip WJ & Daemen FJ (1982). Use of a density modification technique for isolation of the plasma membrane of rod outer segments. *Biochim Biophys Acta* **687**, 296–302.

Kaylor JJ, Yuan Q, Cook J, Sarfare S, Makshanoff J, Miu A, Kim A, Kim P, Habib S, Roybal CN, Xu T, Nusinowitz S & Travis GH (2013). Identification of DES1 as a vitamin A isomerase in Müller glial cells of the retina. *Nat Chem Biol* **9**, 30–36.

Kolesnikov AV, Tang PH, Parker RO, Crouch RK & Kefalov VJ (2011). The mammalian cone visual cycle promotes rapid M/L-cone pigment regeneration independently of the interphotoreceptor retinoid-binding protein. *J Neurosci* **31**, 7900–7909.

Lamb TD & Pugh EN Jr (2004). Dark adaptation and the retinoid cycle of vision. *Prog Retin Eye Res* **23**, 307–380.

Lamb TD & Pugh EN Jr (2006). Phototransduction, dark adaptation, and rhodopsin regeneration. The Proctor Lecture. *Invest Ophthalmol Vis Sci* **47**, 5137–5152.

Lyubarsky AL, Falsini B, Pennesi ME, Valentini P & Pugh EN Jr (1999). UV- and midwave-sensitive cone-driven retinal responses of the mouse: a possible phenotype for coexpression of cone photopigments. *J Neurosci* **19**, 442–455.

Lyubarsky AL, Savchenko AB, Morocco SB, Daniele LL, Redmond TM & Pugh EN Jr (2005). Mole quantity of RPE65 and its productivity in the generation of 11-cis-retinal from retinyl esters in the living mouse eye. *Biochemistry* **44**, 9880–9888.

Makino CL, Taylor WR & Baylor DA (1991). Rapid charge movements and photosensitivity of visual pigments in salamander rods and cones. *J Physiol* **442**, 761–780.

Moiseyev G, Chen Y, Takahashi Y, Wu BX & Ma JX (2005). RPE65 is the isomerohydrolase in the retinoid visual cycle. *Proc Natl Acad Sci U S A* **102**, 12413–12418.

Molday LL & Molday RS (1987). Glycoproteins specific for the retinal rod outer segment plasma membrane. *Biochim Biophys Acta* **897**, 335–340.

Pak WL & Cone RA (1964). Isolation and identification of the initial peak of the early receptor potential. *Nature* **204**, 836–838.

Penn RD & Hagins WA (1972). Kinetics of the photocurrent of retinal rods. *Biophys J* **12**, 1073–1094.

Redmond TM, Yu S, Lee E, Bok D, Hamasaki D, Chen N, Goletz P, Ma JX, Crouch RK & Pfeifer K (1998). Rpe65 is necessary for production of 11-*cis*-vitamin A in the retinal visual cycle. *Nat Genet* **20**, 344–351.

Remtulla S & Hallett PE (1985). A schematic eye for the mouse, and comparisons with the rat. *Vision Res* **25**, 21–31.

Rüppel H & Hagins WA (1973). Spatial origin of the fast photovoltage in retinal rods. In *Biochemistry and Physiology of Visual Pigments*, ed. Langer H, pp. 257–261. Springer-Verlag, New York.

Saari JC (2012). Vitamin A metabolism in rod and cone visual cycles. *Annu Rev Nutr* **32**, 125–145.

Schneeweis DM & Schnapf JL (1999). The photovoltage of macaque cone photoreceptors: adaptation, noise, and kinetics. *J Neurosci* **19**, 1203–1216.

Sullivan JM & Shukla P (1999). Time-resolved rhodopsin activation currents in a unicellular expression system. *Biophys J* **77**, 1333–1357.

Wang JS, Estevez ME, Cornwall MC & Kefalov VJ (2009). Intra-retinal visual cycle required for rapid and complete cone dark adaptation. *Nat Neurosci* **12**, 295–302.

Wang JS & Kefalov VJ (2009). An alternative pathway mediates the mouse and human cone visual cycle. *Curr Biol* **19**, 1665–1669.

Wang JS & Kefalov VJ (2011). The cone-specific visual cycle. *Prog Retin Eye Res* **30**, 115–128.

Wenzel A, Oberhauser V, Pugh EN Jr, Lamb TD, Grimm C, Samardzija M, Fahl E, Seeliger MW, Reme CE & von Lintig J (2005). The retinal G-protein-coupled receptor (RGR) enhances isomerohydrolase activity independent of light. *J Biol Chem* **280**, 29874–29884.

© 2014 The Authors. The Journal of Physiology © 2014 The Physiological Society

Wenzel A, Reme CE, Williams TP, Hafezi F & Grimm C (2001). The Rpe65 Leu450Met variation increases retinal resistance against light-induced degeneration by slowing rhodopsin regeneration. *J Neurosci* **21**, 53–58.

Woodruff ML, Lem J & Fain GL (2004). Early receptor current of wild-type and transducin knockout mice: photosensitivity and light-induced Ca^{2+} release. *J Physiol* **557**, 821–828.

Additional information

Competing interests

None declared.

Author contributions

C.K. and M.T. performed experiments; data were analysed by C.K. and E.N.P. and presented by C.K. C.K., M.E.B. and E.N.P. designed the experiments and wrote the paper.

Funding

This work was supported by the National Eye Institute (R01EY02660 to E.N.P. and R01EY14047 to M.E.B.).

Acknowledgements

The authors are very grateful for the thoughtful comments of the reviewers.

© 2014 The Authors. The Journal of Physiology © 2014 The Physiological Society